Radiation Performance of Low Bend-Loss Optical Fiber for Gyroscope Applications

T. Geisler, R.V.S. Jensen, J.O.Olsen, B. Palsoditer
OFS
Brøndby, Denmark
tgeisler@ofsoptics.com

J. Fini, M. LuValle
OFS Laboratories
OFS
Somerset, NJ USA
mjl@ofsoptics.com

E. J. Friebele
Naval Research Laboratory
Washington, DC USA
friebele@nrl.navy.mil

Abstract— **In this presentation we will describe the effect of radiation on a low bend loss, polarization maintaining (PM) fiber for an interferometric fiber optic gyroscope (IFOG). Our experimental design for exploring radiation effects incorporated unusual steps up and down in temperature during irradiation in order to further elucidate the radiation darkening mechanism. While the experiments showed that the fiber was radiation hard, and the step had the desired effect of increasing the statistical precision of the model, it also showed the surprising result that in addition to accelerating the annealing of defects, increased temperature accelerates the formation of loss-causing defects during irradiation.**

Keywords—Polarization maintaining fiber, Radiation sensitivity)

I. INTRODUCTION

The PM fiber we study here has a pure silica core with boron-doped stress rods in a PANDA like design and a typical beat length of 5 mm. The fiber diameter is 80 µm enabling very compact IFOG coil construction. The operating wavelength is 1550 nm and the typical intrinsic attenuation is 0.4 dB/km with a cutoff wavelength of 1450 nm and a mode field diameter of 8.9 µm. The improved bend performance is achieved by a depressed cladding index profile. The bend performance typically results in an additional bend loss of less than 0.05 dB/turn on a 12 mm mandrel at 1600 nm. The radiation performance is optimized through the preform design and draw conditions. The beat length is measured at the operating wavelength (1550 nm), and the h-parameter is below $2*10^{-4}$ in a 20 mm coil configuration over a broad temperature range.

The radiation experiment was designed to use a reasonably small number of runs, yet allow extrapolation to arbitrary temperature dose-rate time trajectories. The irradiation was done at the gamma irradiation facility at NRL. The experiments are part of a factorial design, considering only the dose rate and total dose as two factors. The two values of the dose rate factor are 0.97 rad/sec (L) and 135 rad/sec (H), and the total dose values are 100 krads (l) and 1 Mrad (h). The three experiments are:

1. Ll: Exposure at 35 C followed by a 500 hour anneal at 35 C
2. Hl: Exposure at 35 C followed by a 500 hour anneal at 35 C
3. Hh: First half of the exposure at 35 C, next one third at 50 C, and final sixth at 35 C followed by 500 hour anneal at 35 C.

The temperature step-stress portion of the final experiment was planned to allow us to get an accurate measure of the effect of temperature on annealing behavior. The analysis was done using tools described elsewhere [1, 2]. The major assumptions in the analysis are that there are

- One or more classes of defect
- Within each class, radiation-induced loss is proportional to the concentration of defects.
- The growth in concentration of defects follows a power law in dose rate.
- The annealing of defects occurred as if it were an nth order chemical process n≥1, assuming a distribution of activation energies across sites in the glass.

In the next section, the experiment is described in detail, the third section discusses analysis and the last summarizes results.

II. EXPERIMENT

The fiber samples were exposed to ^{60}Co γ-rays at the Naval Research Laboratory cobalt pool facility. Either 200 m

(Hh, Hl) or 400 m (Ll) of fiber was wound on a paper form 2" in diameter which was placed inside a double-wall stainless steel sample can. The fiber leads were run though a small hole in the sample can lid. The hole was sealed with silicone, and the fibers were fusion-spliced to a duplex fiber cable that ran from the source up to the test set. The light source was an Agilent 83437A broadband source with 4 EELEDs centered at 1310, 1430, 1550, and 1650 nm. An Ando 6317A OSA acquired spectral data from 1250 to 1750 nm. Since data were to be acquired simultaneously from all 3 fibers, a JDSU 2 x 24 SB series fiber optic switch was used to interrogate each fiber in turn. As part of each measurement sequence, a source reference spectrum was obtained using a loop-back channel. Normalizing each fiber spectrum by the loop-back reference eliminated any influence of light source fluctuations. The data rate at the beginning of the exposure and the end of exposure and beginning of the recovery periods was the maximum possible, ~7 s per point, but the rate was slowed to as much as 15-30 min during recovery. A LabView program controlled the switches and the temperature of the coil in the sample can via a thermocouple and heater and acquired spectra from the OSA. The induced absorption as a function of wavelength and time (or dose) was calculated by subtracting a spectrum taken prior to exposure from the spectra during exposure or recovery.

The growth of the radiation-induced loss was measured during the exposure period, and then recovery was measured for ~2.5 x 10^6 s. Approximately one day after the end of the exposure, the fiber coil was removed from the sample can and placed in an oven at 35 C where it remained for the remainder of the recovery period. This procedure, which lasted ~10 min during which the fiber returned to room temperature and no data were taken, required re-splicing the fiber leads. Although re-splicing caused an offset in the induced loss, it could be subtracted out, resulting in smooth data over the full ~25 day recovery period.

III. Analysis

The software used in the analysis was originally developed for general analysis for accelerated testing [1] and then specialized to the analysis of radiation damage in optical fibers [2]. Further modification has been undertaken for the experiments reported here. The main purpose of the software was to allow engineers to fit models based on the differential equations used in chemical kinetics as a way of approximating observed degradation and failure processes. One of the main ways to achieve this is to divide a period of constant stress into evenly spaced epochs, so that the integrations are easily and quickly performed. Concentrations of defects of different classes and sub classes (for example different activation energies for annealing) are kept track of, then summed to come up with total darkening, adapted to each wavelength.

Data are fit simultaneously to all experiments at multiple wavelengths, so the model parameters are self consistent across multiple views of the data. Departures of the model from the data show potential departures of the model from reality. One detail not included in the analysis here is the problem of transients and uncertainty about time over which the environment is changing. Typically, when the environment is changed during an experiment it occurs between measurements. The exact time is often not recorded, and usually it is estimated to optimize fits. This has not been done yet here, instead assuming for example that the irradiation stopped precisely at the last measured time during irradiation, and that the temperature rise started precisely on a given time measurement. Based on the data acquisition rate, this could introduce an error of up to ~8 s.

The original intent of the step-stress in temperature during the middle of the high dose rate, high dose radiation exposure shown in Figure 1 was to allow estimation of the effect of temperature on annealing rate. Otherwise, the experiment followed the pattern we used before [2] in studying dose rate and annealing effects. In particular we examined practically-achievable variations in dose rate and total dose given the time we had for the experiment, and chose the two experiments at high dose rate to examine high dose and low dose effects, then examined only the low total dose at the low dose rate due to practical issues of finishing the experiment in reasonable time.

What we did expect was that the temperature step would result in an easy to distinguish drop and further rise at lower rate during the temperature step when displayed in log time, as simulations showed. In fact the drop is nearly invisible, and it is not clear that the subsequent rise is any slower. The simplest adjustment (in order to be consistent with the model of glass defects obeying kinetic laws) that we could make in order to account for the data was to assume that higher temperature accelerated the growth in defects.

In order to fit the times when the temperature was changing (during the steps), the temperature change was discretized into 21 steps, including beginning and ending temperature. For the 1st order model, 21 discrete rate matrices were calculated, and the one with temperature closest to that observed for the time step was used to modify the defect concentrations. Figure 1 below shows why, particularly for the drop in temperature from 50 C back to 35 C taking more than ½ hour, it was necessary to do a good approximation of the ramping in temperature. It also shows that the temperature was nearly stabilized at the end of irradiation. The anneal was divided into 3 time periods: 1st half hour, next 9.5 hours, and the remainder, and each time period was represented by 200 points in order to catch the early changes during anneal.

Figure 2 below shows the 1st order kinetic fits, without any temperature dependence included. Even though fits on the the linear time plots look fairly good, it is clear from the log time plots that there is significant departure of the model from the data. However, the data does show one characteristic that is important. The peak loss is highest at short wavelengths, but the persistent tail from anneal is highest

at long wavelengths. This is only possible if there are two (or more) classes of defects, one showing up more at short wavelengths and one showing up more at long wavelengths.

Figure 3 shows the 1st order fit with a temperature dependence. Visually we can see the fit lines do better at lining up with the center of the data, and an F test of the residual with 3 and 678 degrees of freedom gives a value of well over 1000, indicating a clearly better fit (P=0).

Figure 4 shows the nth order fits (n allowed to vary from 1 up, with a temperature dependence built in). Here because of the nonlinear nature of the anneal, every temperature fluctuation during the ramp influenced the anneal rate. However beyond that, the nth order anneal (when n was not allowed to collapse to 1) shows clear departure from the observed behavior.

Using the first order model, extrapolations were calculated assuming 20 mm of aluminum shielding for the gyro [4], over a 20 year geosynchronous orbit. We assumed 3 major solar flares per decade distributed randomly across the 20 years, with random durations and with a maximum dose rate of 1 rad/sec at the fiber. The total accumulated dose from the solar flares was designed to be 60 krad, which is approximately 50% more than assumed will occur [4].

The resultant prediction is shown below in Figure 5. We see that the maximum radiation-induced loss at 1550 nm is just over 1 dB/km immediately after the large flare about quarter way through the two decade time span. The baseline incremental loss rises approximately 0.2 dB/km throughout the life of the fiber, due to the unannealed tail from each flare.

Figure 1

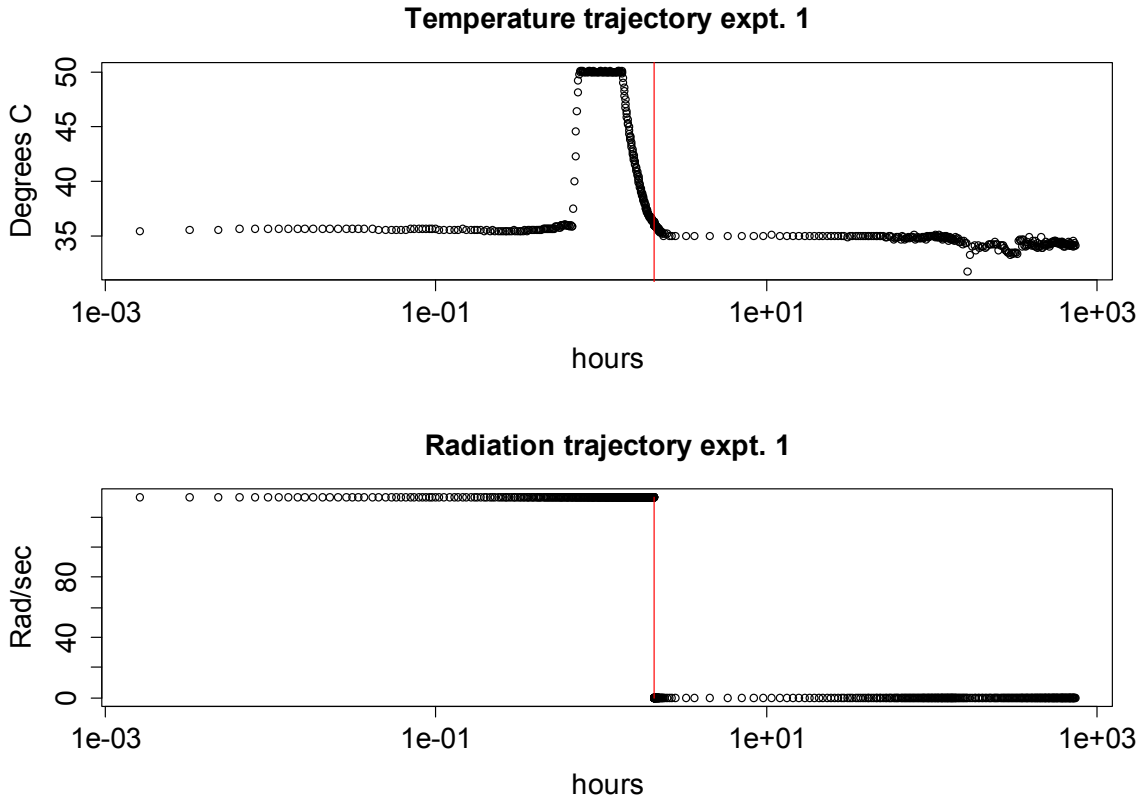

Fig. 1. Figure 1 above shows the temperature and radiation dose rate trajectories for the high dose rate-high total dose experiment. The red line shows the end of radiation in both the temperature and dose rate plot.

Figure 2, 1st order fits, no temperature dependence

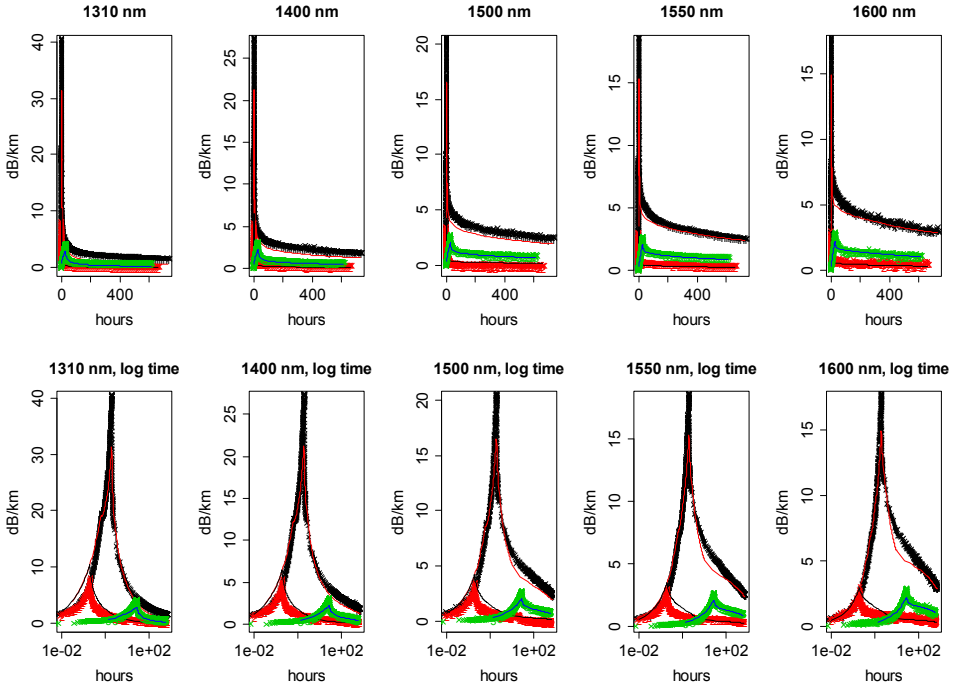

Fig. 2. Top plots show radiation-induced loss vs. time plotted on a linear scale; bottom plots show log time. Each column is a different wavelength. Symbols are data, fits are lines. To allow the fits to be seen, red lines are used with black symbols, black lines with red symbols, and blue lines with green symbols. Black symbols are data from the Hh experiment, red symbols are data from the Hl experiment and green symbols are data from the Ll experiment.

Figure 3 1st order fits, includes temperature dependence

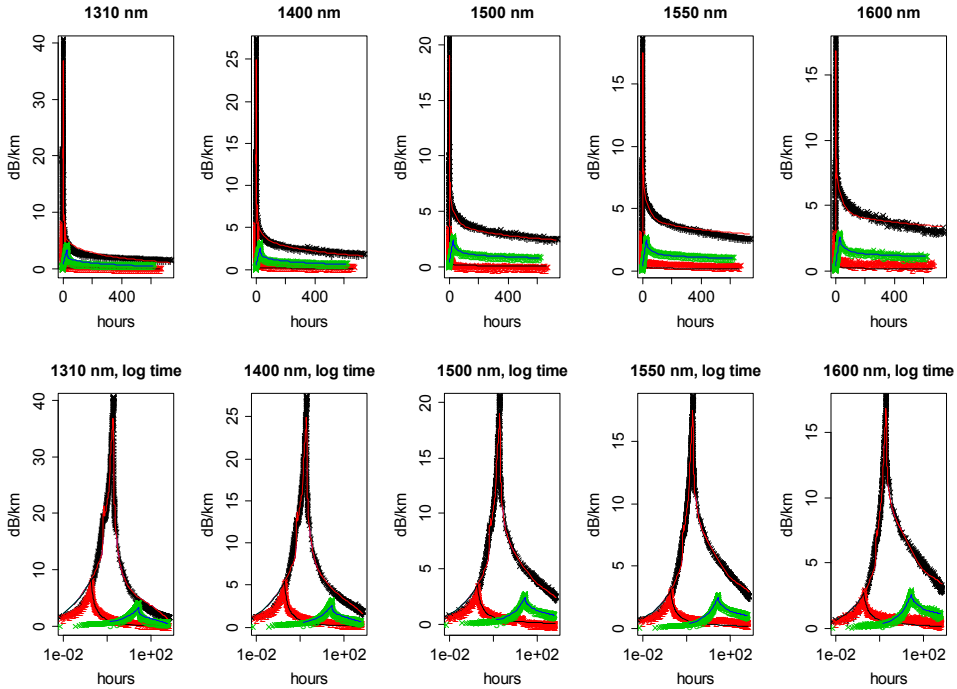

Fig. 3. As in figure 2, Symbols are data, fits are lines. To allow the fits to be seen, red lines are used with black symbols, black lines with red symbols, and blue lines with green symbols. Black symbols are data from the Hh experiment, red symbols are data from the Hl experiment and green symbols are data from the Ll experiment

Figure 4 nth order fits, includes temperature dependence

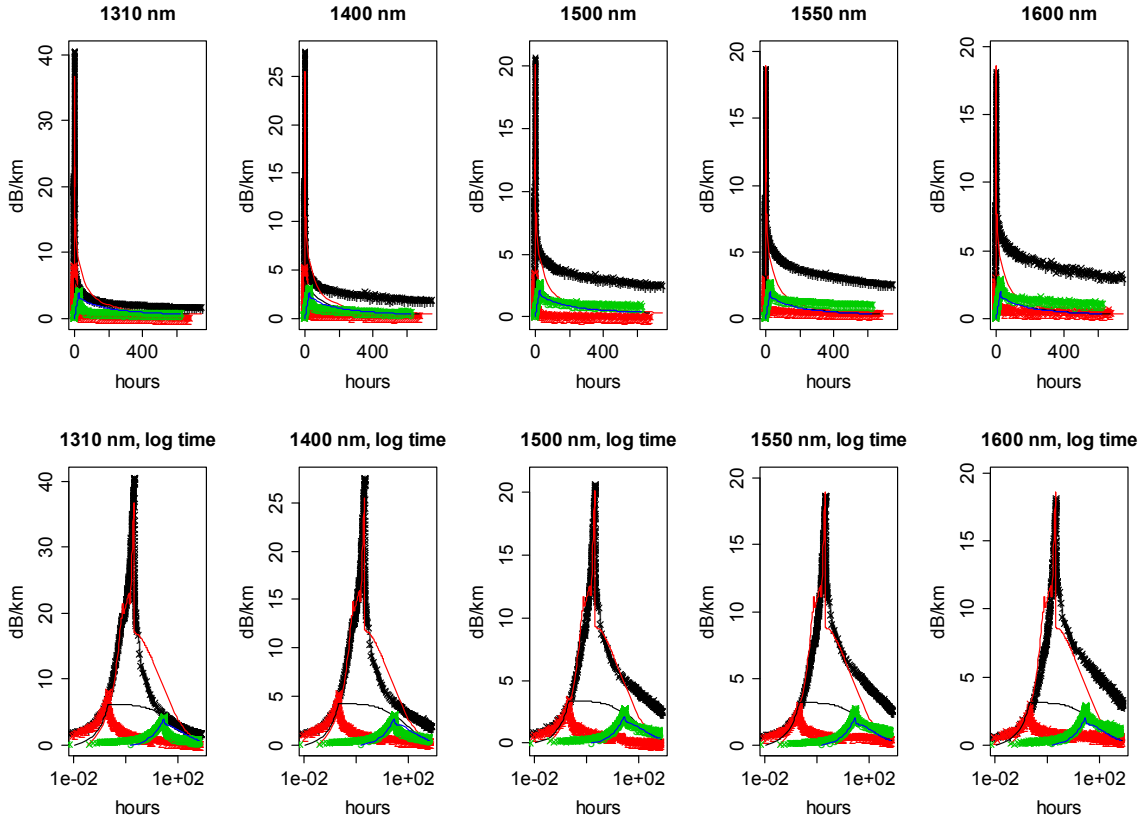

Fig. 4. As in figure 2, Symbols are data, fits are lines. To allow the fits to be seen, red lines are used with black symbols, black lines with red symbols, and blue lines with green symbols. Black symbols are data from the Hh experiment, red symbols are data from the Hl experiment and green symbols are data from the Ll experiment

Figure 5

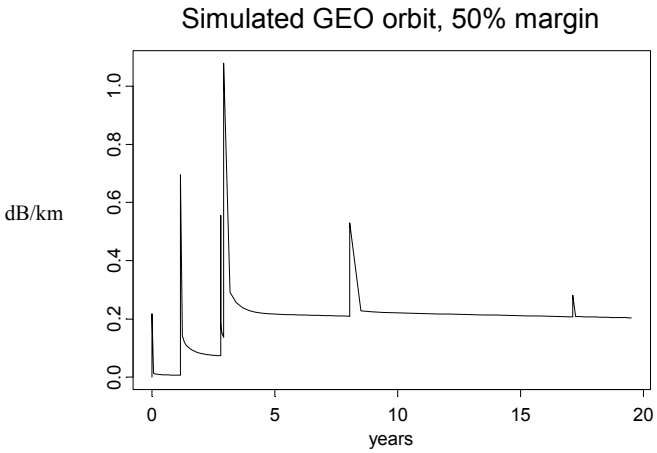

Fig. 5. Radiation-induced incremental loss vs. time on orbit. Flares were simulated assuming 4 major flares per decade over two decades with a total exposure of 60 Krad (50% more than assumed from standard exposure with 20 mm of Al shielding in a Geosynchronous orbit[4]). Flare timing was chosen from order statistics of a uniform random variable, flare spacing from an independent sample of differences between order statistics of a uniform random variable so total dose added to 60 Krad.

IV. RESULTS

Our main results to date are:

1. The fiber is quite radiation-hard,
2. There are clearly two classes of defects,
   a. One with a greater effect at shorter wavelengths and having less persistence
   b. A second affecting the longer wavelengths and lasting longer.
3. The generation rate of radiation-induced defects, in addition to depending on dose rate, also depends on temperature. This dependence operates in a way to work against the annealing process, i.e. the higher the temperature, the higher the growth rate.

The last result is quite significant. This complexity in temperature irradiation combination has been observed [5] elsewhere, but this is in significantly lower temperature conditions. Most models of radiation darkening assume thermal annealing which is independent of the growth

process. The fact that we achieved a better fit under the assumption that the growth part of the kinetics could be thermally accelerated shows that simply annealing at multiple temperatures is not sufficient for identifying the dynamics of radiation-induced darkening in fibers, and can result in the erroneous conclusion that raising the temperature during irradiation will reduce the final loss more than it actually will. The confidence bounds generated by the model were also much tighter than we expected. Visually, they are nearly coincident with the estimate, which comparing to [2] shows that the statistical design is significantly better. Thus, we are seeing preliminary evidence that temperature changes during exposure are in fact more efficient for identifying dynamics.

REFERENCES

[1] LuValle, M., LeFevre, B, and Kannan, S.., (2004), Design and analysis of accelerated tests for mission critical reliability, CRC Chapman Hall, Boca Raton

[2] LuValle et al., (2006), "Radiation Induced Loss Predictions for Pure Silica Core Polarization Maintaining Fibers" SPIE 6193-50

[3] Benson (1960), Foundations of chemical kinetics, McGraw Hill, New York

[4] Poizat, M. (2009). "Space Environment and Effects", Internet [Online]. Available: http://space.epfl.chwebdav/site/space/shared /industry_media/02% 20EPFL_space_environment. pdf Jun, 9.

[5] Girard et al (2013), "Combined High dose and temperature radiation effects on Multimode silica based optical fibers", IEEE Transactions on Nuclear Science, V60 #6, pp4305-4313